

# Fiber Supercapacitors Made of Nanowire-Fiber Hybrid Structures for Wearable/Flexible Energy Storage\*\*

Joonho Bae, Min Kyu Song, Young Jun Park, Jong Min Kim,\* Meilin Liu, and Zhong Lin Wang\*

Recently, there has been great interest in flexible and wearable energy devices for applications in flexible and stretchable electronics. Even though future developments are moving toward thinner, lighter, and cheaper solutions,<sup>[1,2]</sup> many existing energy-harvesting and storage devices are still too bulky and heavy for intended applications. For example, high-efficiency dye-sensitized solar cells (DSSCs) employ fluorine-doped tin oxide (FTO) glass as the substrate of working electrode. However, the use of rigid FTO glass has restricted adaptability of DSSCs during transportation, installation, and application,<sup>[2]</sup> requiring further development of flexible cells to improve DSSC adaptability. To develop flexible and wearable electronics, not only new materials for the substrates used in energy storage devices such as batteries and supercapacitors need to be explored, but future development of higher performance energy systems still depends on the employment of new and lighter electrode materials.

In recent years, electrochemical supercapacitors have attracted much attention as novel energy-storage devices because of their high power density, long life cycles, and high efficiency.<sup>[3–12]</sup> Supercapacitors can deliver higher power than batteries and store more energy than conventional capacitors.<sup>[13,14]</sup> Current research on supercapacitors has focused on their applications in electric vehicles, hybrid electric vehicles, and backup energy sources. Thus, conventional supercapacitors are heavy and bulky, and it is still a challenge to achieve high efficiency miniaturized energy-storage devices that are compatible with the flexible/wearable electronics.<sup>[15]</sup>

Herein, we present a prototype of a high-efficiency fiber-based electrochemical microsupercapacitor using ZnO nanowires (NWs) as electrodes. These fiber supercapacitors, which have great potential for scale-up, comprise two electrodes that employ a flexible plastic wire and a Kevlar fiber as a substrate. Both wire and fiber are covered with arrays of high-quality ZnO NWs grown by the hydrothermal method, and ZnO NWs on a Kevlar fiber was coated with a thin gold film

to improve the charge-collection capacity. Furthermore, employment of ZnO NWs could provide exciting solutions to the future development of wearable energy devices. Our fiber-based microsupercapacitor would be large enough to be used in self-powering nanosystems, such as a power shirt using piezoelectric ZnO NWs grown radially around textile fibers.

Even though conventional research efforts on bulky supercapacitors have focused on the use of carbon-based materials, such as activated carbons, and some transition metal oxides, such as RuO<sub>2</sub> and ZnO, could have several advantages over the conventional electrode materials of supercapacitors for the wearable electronics. First, it can be grown at low temperatures (less than 100 °C) by a chemical approach on any substrate and any shape substrate. Second, it is biocompatible and environmentally friendly material. Furthermore, ZnO NWs<sup>[16–20]</sup> can provide large specific surface area, which is crucial to high-efficiency supercapacitors. Compared with other oxide materials, ZnO NWs can be grown easily on fibers or textures at low temperatures (less than 90 °C). Using this unique advantage of ZnO NW growth, we have demonstrated NW nanogenerators that can scavenge energy from the environment by using fabrics.<sup>[16]</sup> The fiber supercapacitors presented herein could be combined with the fiber nanogenerators, possibly enabling us to achieve a wearable power system. In the future nanosystem, it will be necessary to store energy, especially when an intermittent energy source (such as ZnO-based nanogenerators) is used.<sup>[21]</sup> Fiber supercapacitors could enable us to store electrical energy that is converted from mechanical energy by simple mechanical vibration, such as light wind, footsteps, and heartbeats.

Figure 1a shows a low-magnification SEM image of a poly(methyl methacrylate) (PMMA) plastic wire covered with ZnO NWs along with a close-up view (Figure 1b). The wire is highly flexible, and its diameter is about 220 μm. The as-grown ZnO NWs on the plastic wire show typical hexagonal flat-ended morphology of ZnO NWs, which grow almost vertically on the substrate of plastic wire. The NW diameters range from 500 nm to 700 nm, and the lengths are about 6 μm.

The fiber-based electrochemical capacitor (Figure 1c) was assembled by entangling a plastic wire covered with NWs around a Kevlar fiber covered with gold-coated NWs. For the entangling process, the plastic wire was placed on a stage, and the Kevlar fiber was entangled carefully by using tweezers. The resistance of the device was monitored during the entangling process to ensure the two electrodes were not in contact each other. As shown in the results of electrochemical measurements (see below), the liquid or gel electrolytes seem to play a role in separating the two electrodes, and contact

[\*] Dr. J. Bae, M. K. Song, Prof. M. Liu, Prof. Z. L. Wang  
School of Materials Science and Engineering  
Georgia Institute of Technology, Atlanta, GA 30332 (USA)  
Fax: (+1) 404-385-3852  
E-mail: zlwang@gatech.edu  
Dr. Y. J. Park, Dr. J. M. Kim  
Frontier Research Lab, Samsung Electronics  
Gyeonggi-Do, 446-712 (South Korea)  
Fax: (+82) 31-280-9349  
E-mail: jongkim@samsung.com

[\*\*] Research supported by Samsung Electronics, Inc. Z.L.W. thanks the partial support of WCU administrated by UNIST.

Supporting information for this article is available on the WWW under <http://dx.doi.org/10.1002/anie.201006062>.

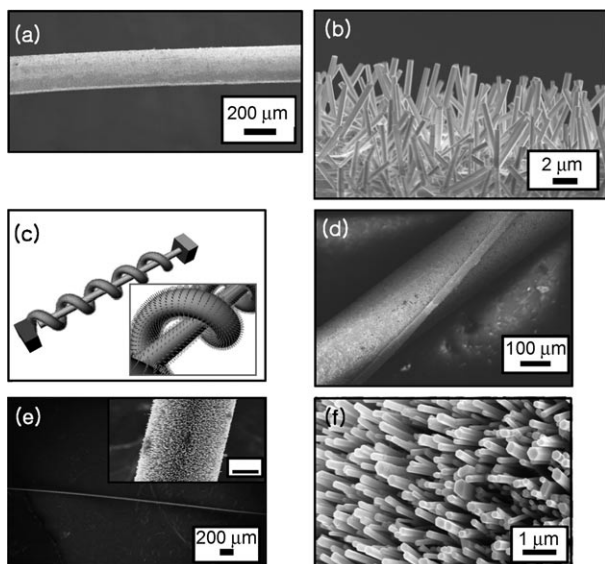


**Figure 1.** a) Low-resolution SEM image of a gold-coated plastic wire covered with ZnO NW arrays. b) Higher-magnification SEM image of the plastic wire, showing arrays of NWs. c) A fiber-based supercapacitor. d) Low-resolution SEM image of fiber supercapacitors consisting of entangled Kevlar fiber and plastic wire. e) Low-resolution SEM image of a Kevlar fiber covered with ZnO NW arrays. Inset: Close-up; scale bar: 10  $\mu\text{m}$ . f) Higher-magnification SEM image of the fiber, showing ZnO NW arrays grown along the radial direction.

events between the two electrodes were very rare in the devices with electrolytes.

The typical number of turns of twisting Kevlar fiber around plastic wire was 5, and the active length of the plastic wire in which the plastic wire and Kevlar fiber are entangled to form the supercapacitor was 5 mm. The space between the NWs is of the order of several hundred nanometers. The area of the capacitor in which two electrodes (wire and fiber) are entangled was immersed in 1M  $\text{KNO}_3$  aqueous electrolyte solution. The SEM image of the area in which two electrodes are entangled is shown in Figure 1 d.

The electrochemical properties of the capacitors in 1M  $\text{KNO}_3$  aqueous electrolyte solution were characterized using a potentiostat/galvanostat (Princeton Applied Research VersaStat 3F). Cyclic voltammetry shows that our device has a good electrochemical stability and the capacitance of fiber-based electrochemical capacitors (Figure 2a). The scan range is between 0 and 500 mV with scan rates of 5, 20, and 100  $\text{mVs}^{-1}$ . The galvanostatic charge–discharge measurement was also conducted to characterize the electrochemical capacitor performance of the fiber supercapacitors, and the curve is shown in Figure 2b. To obtain this curve, the charge–discharge current was kept constant at 1  $\mu\text{A}$ . The typical triangular shape of these charge–discharge curves suggests that the capacitance of our fiber supercapacitors originates from the effective ion adsorption at the interface of electrolyte/ZnO NWs.

The capacitance as a function of potential at a voltage scan rate of 100  $\text{mVs}^{-1}$  is shown in Figure 2c. The capacitance can

be calculated from cyclic voltammograms (Figure 2a) using the equation of  $C = Q/V = I/S$ , where  $C$  is the capacitance,  $Q$  is the charge accumulated in the capacitors,  $V$  is the potential in the CV curve,  $I$  is the current in the CV curve, and  $S$  is the scan rate ( $\text{Vs}^{-1}$ ). It can be seen that the capacitance ranges from 0.006 to 0.007 mF. To compare the capacitance values to other supercapacitors that have been reported, we calculated area specific capacitance (Figure 2d, upper). This area-specific capacitance curve reveals that the specific capacitance of fiber supercapacitors in 1M  $\text{KNO}_3$  reached values of up to about 0.21  $\text{mFcm}^{-2}$  at the voltage scan rate of 100  $\text{mVs}^{-1}$ .

Conventional electrochemical capacitors have two-dimensional plate-like substrates. As our fiber supercapacitors have unique one-dimensional substrates, capacitance per unit length ( $\text{mFcm}^{-1}$ ) would be a useful parameter to characterize the capacitance behavior of the devices. In this regard, we calculated the capacitance per unit length by dividing the capacitance in Figure 2c by the effective length of the device (5 mm). The bottom Figure in Figure 2d reveals that the capacitance per unit length reached up to about 0.02  $\text{mFcm}^{-1}$ . Microsupercapacitors were reported to have an area-specific capacitance of 0.4–2  $\text{mFcm}^{-2}$ ,<sup>[22–25]</sup> indicating that the capacitance value of 0.21  $\text{mFcm}^{-2}$  of our device in 1M  $\text{KNO}_3$  is slightly lower than those in the literature. Further optimization would be necessary to increase the specific capacitances of fiber supercapacitors. For instance, matching

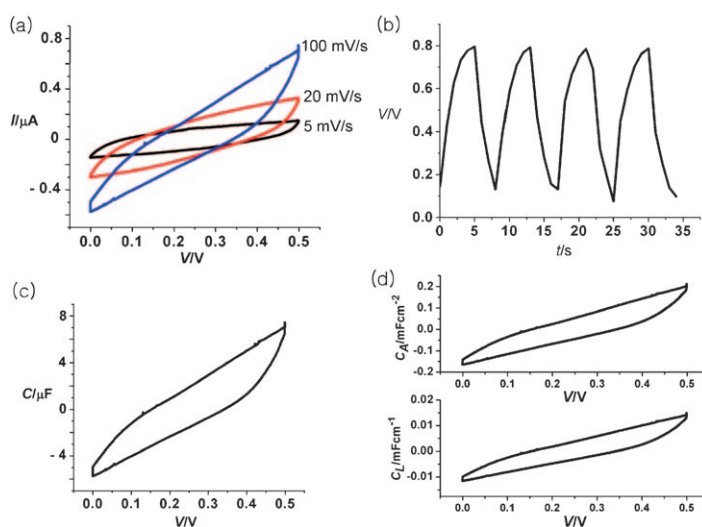


**Figure 2.** a) Typical cyclic voltammograms of a fiber supercapacitor. Electrolyte: 1M  $\text{KNO}_3$ . b) Galvanostatic charge–discharge curve measured at 1  $\mu\text{A}$ . c) Cyclic voltammogram of a fiber supercapacitor in 1M  $\text{KNO}_3$  electrolyte. Scan rate: 100  $\text{mVs}^{-1}$ . d) Top: Area-specific capacitance  $C_A$  of the fiber supercapacitors at 100  $\text{mVs}^{-1}$ . Bottom: Length-specific capacitance  $C_L$  of the fiber supercapacitors at 100  $\text{mVs}^{-1}$ .

the pore sizes and solvated ion sizes of electrolytes, and controlling the density of ZnO NWs,<sup>[26]</sup> is very critical to obtain the high performance of electrochemical capacitors. For practical applications, we explored the possibility of increasing the capacitance value of our devices.

To enhance the specific capacitance of fiber-based supercapacitors, we coated ZnO NWs grown on plastic wires with

MnO<sub>2</sub> to employ the large pseudocapacitances of MnO<sub>2</sub>.<sup>[27,28]</sup> MnO<sub>2</sub> was successfully deposited by the reduction of MnO<sub>4</sub><sup>-</sup> by ethanol at room temperature (see Experimental Section).<sup>[29]</sup> The capacitance of single wire was measured by cyclic voltammetry (CV) in a conventional three-electrode system. The ZnO NWs grown on wire before and after MnO<sub>2</sub> coating were used as working electrodes. A Pt wire and a saturated calomel electrode (SCE) were used as a counter electrode and a reference electrode, respectively. The CV measurements were performed in the 1M Na<sub>2</sub>SO<sub>4</sub> solution between 0 and 0.8 V (vs. SCE) with a voltage scan rate of 100 mVs<sup>-1</sup>.

As shown in Figure 3, the specific capacitance of this energy storage device reached up to 2.0 mFcm<sup>-2</sup> at 100 mVs<sup>-1</sup>, which is comparable to values reported for electrochemical microsupercapacitors (0.4–2 mFcm<sup>-2</sup>),<sup>[22–25]</sup> as mentioned above. Figure 3 also shows that the MnO<sub>2</sub> coating significantly enhanced specific capacitances (an over 20-fold increase of area specific capacitance after MnO<sub>2</sub> coating). This result indicates that the performance of our fiber supercapacitors could be further enhanced by using the optimized MnO<sub>2</sub> coating.

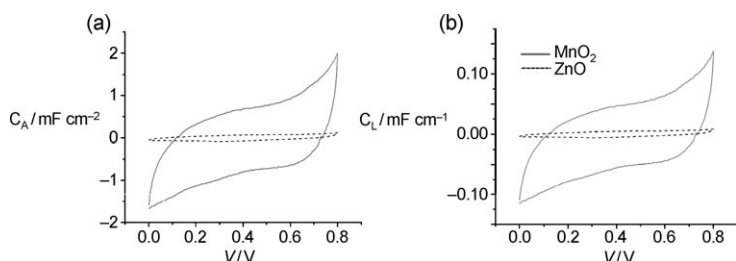


**Figure 3.** a) Area-specific capacitance of ZnO NWs on a plastic wire before (----) and after MnO<sub>2</sub> coating (—). Scan rate: 100 mVs<sup>-1</sup>. b) Length-specific capacitance of ZnO NWs on a plastic wire before (----) and after MnO<sub>2</sub> coating (—). Scan rate: 100 mVs<sup>-1</sup>.

Recently, solid gel electrolytes have been explored as alternative electrolytes of conventional liquid electrolyte in electrochemical devices. Solid gel or polymer electrolytes were reported to combine the separator and the electrolyte into a single layer, whereas liquid electrolytes require a separator to avoid electrical contact between the electrodes. To make our fiber supercapacitors fully wearable, the electrolyte needs to be fully encapsulated in the devices without any leakage. In this regard, use of solid gel electrolytes are more preferable than liquid electrolytes of KNO<sub>3</sub> for future applications of fiber supercapacitors.

To test the performance of the gel electrolytes in our fiber supercapacitors, we performed the electrochemical measurements of fiber supercapacitors using a gel electrolyte instead of KNO<sub>3</sub> liquid electrolytes. The fiber supercapacitors in the gel electrolyte was fabricated and measured under the same process as the supercapacitors in KNO<sub>3</sub> electrolytes. Poly(vinyl alcohol) (PVA) powder (10 g) mixed with water (100 mL) and phosphoric

acid (10 g) was used as the gel electrolyte. Figure 4a shows cyclic voltammograms of the fiber supercapacitors with the gel electrolyte. The scan rate ranges from 10 to 200 mVs<sup>-1</sup> with a scan rates of 5, 20, and 100 mVs<sup>-1</sup>. The good capacitive behavior of the supercapacitors with gel electrolytes (PVA/H<sub>3</sub>PO<sub>4</sub>) is clearly seen. A galvanostatic charge–discharge curve for PVA/H<sub>3</sub>PO<sub>4</sub> is also shown (Figure 4b). The discharge current was 2 μA. The area-specific capacitance curve also reveals that the fiber supercapacitors in PVA/H<sub>3</sub>PO<sub>4</sub> demonstrated specific capacitance of about 2.4 mFcm<sup>-2</sup> at the voltage scan rate of 100 mVs<sup>-1</sup> (Figure 4d).

The improvement of internal resistance of fiber supercapacitors using the gel electrolytes is noteworthy. The  $iR$  drop in the charge–discharge curves for KNO<sub>3</sub> electrolyte was about 0.3 V (Figure 2b). When the gel electrolyte was used for fiber supercapacitors, the  $iR$  drop was reduced to 0.06 V (Figure 4b), indicating that the internal resistance was significantly lowered by the gel electrolytes. Electrochemical impedance spectroscopy (EIS) measurement reveals that the internal resistance of the supercapacitors with gel electrolyte is about 1.05 Ωcm<sup>2</sup> (see the Supporting Information).

The energy density  $E$  of fiber supercapacitors in the gel electrolytes can be calculated using Equation (1):

$$E = 0.5 C V^2 \quad (1)$$

where  $V$  is the operating voltage and  $C$  is the specific capacitance of the fiber supercapacitor. In the galvanostatic charge–discharge curve (Figure 4b), the operating voltage is 0.29 V. Thus, the energy density of the fiber supercapacitor in gel electrolyte is about  $2.7 \times 10^{-8}$  Whcm<sup>-2</sup>. The power density can be

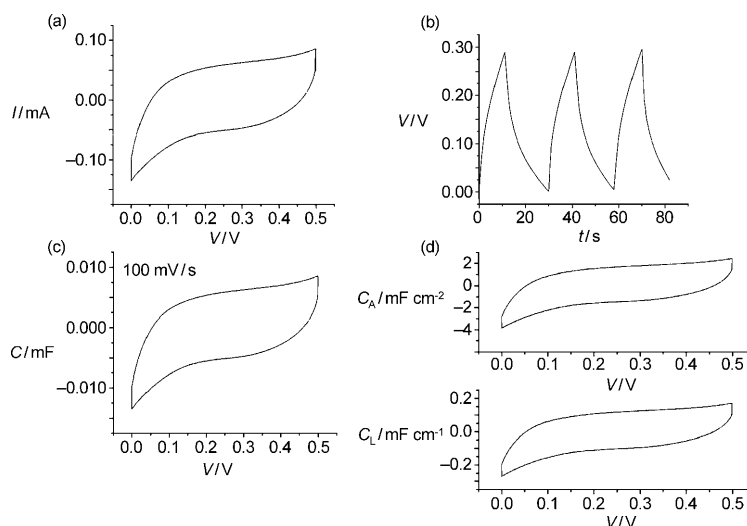


**Figure 4.** a) Typical cyclic voltammogram of a fiber supercapacitor using a PVA/H<sub>3</sub>PO<sub>4</sub> gel electrolyte. Scan rate: 100 mVs<sup>-1</sup>. b) Galvanostatic charge–discharge curve measured at 2 μA. c) Cyclic voltammogram of a fiber supercapacitor in the gel electrolyte. Scan rate: 100 mVs<sup>-1</sup>. d) Top: Area-specific capacitance of the fiber supercapacitors. Scan rate: 100 mVs<sup>-1</sup>. Bottom: Length-specific capacitance of the fiber supercapacitors. Scan rate: 100 mVs<sup>-1</sup>.

obtained by dividing the energy density by the discharge time (7 s) in Figure 4b. Thus, the power density is  $1.4 \times 10^{-5} \text{ W cm}^{-2}$ .

The power densities of carbon-based supercapacitors reported by other groups range from  $10^{-3}$  to  $10^{-1} \text{ W cm}^{-2}$ , and the energy densities are  $10^{-6}$ – $10^{-4} \text{ Wh cm}^{-2}$ .<sup>[3]</sup> The power density and energy density of our fiber supercapacitors in the gel electrolytes are significantly lower compared to typical carbon-based supercapacitors. However, the power density and energy density could be further improved by incorporating more fibers in the device or scale-up process. We also expect that the low values of power density and energy density could be improved and optimized by the use of  $\text{MnO}_2$  coating.

A comparison of specific capacitances of fiber supercapacitors with three different configurations ( $\text{ZnO}$  NWs in two different electrolytes of  $\text{KNO}_3$  and  $\text{PVA}/\text{H}_3\text{PO}_4$ , and  $\text{MnO}_2$  coating in  $\text{Na}_2\text{SO}_4$  electrolyte) is presented in Figure 5.

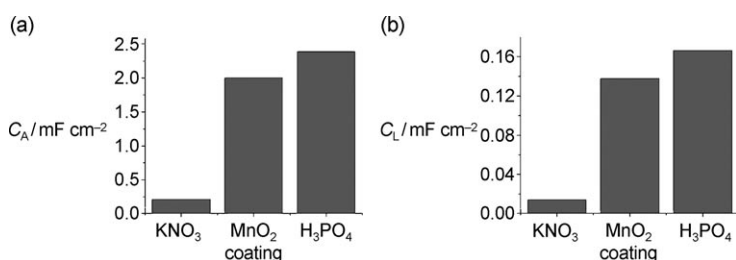


**Figure 5.** Comparison of specific capacitances of fiber supercapacitors with three different configurations ( $\text{ZnO}$  NWs in  $\text{KNO}_3$  and  $\text{PVA}/\text{H}_3\text{PO}_4$  electrolytes, and  $\text{MnO}_2$  coating in  $\text{Na}_2\text{SO}_4$  electrolyte).

Under the same set-up and fabrication process as fiber supercapacitors with  $\text{KNO}_3$ , the gel electrolytes ( $\text{PVA}/\text{H}_3\text{PO}_4$ ) resulted in a specific capacitance ( $2.4 \text{ mF cm}^{-2}$ ) that is ten times higher than the aqueous electrolytes ( $0.21 \text{ mF cm}^{-2}$ ) at the voltage scan rate of  $100 \text{ mV s}^{-1}$ . The gel electrolyte is much more convenient than any aqueous electrolytes, such as  $\text{KNO}_3$ . The gel electrolyte has also demonstrated higher specific capacitances compared to  $\text{MnO}_2$ -coated  $\text{ZnO}$  NWs in  $1 \text{ M Na}_2\text{SO}_4$  solution ( $2.0 \text{ mF cm}^{-2}$ ). This observation and higher specific capacitances using the gel electrolytes suggest that the gel electrolytes not only could be useful for fully wearable fiber supercapacitors, but are also promising as high-efficient fiber supercapacitors.

In conclusion, we have successfully demonstrated novel wearable microsupercapacitors with high specific capacitances. This electrochemical energy storage device was fabricated by using Kevlar fibers and flexible plastic wires as substrates for  $\text{ZnO}$  NW arrays. Using two fiber-based electrodes and  $1 \text{ M KNO}_3$  as an electrolyte, the supercapacitors exhibited specific capacitances of  $0.21 \text{ mF cm}^{-2}$  and  $0.01 \text{ mF cm}^{-1}$ . The specific capacitances of fiber-based supercapacitors can be further enhanced at least twentyfold by using  $\text{MnO}_2$  coatings. When the electrolyte was replaced with a gel electrolyte of  $\text{PVA}/\text{H}_3\text{PO}_4$ , the gel electrolyte showed high specific capacitances of  $2.4 \text{ mF cm}^{-2}$  and  $0.2 \text{ mF cm}^{-1}$ .

This successful demonstration of capacitance behavior using the gel electrolytes suggests the possibility of fully incorporating electrolytes to any fibers or fabrics. The fiber supercapacitors can be easily scaled-up (to the level of normal supercapacitors) to meet the power and energy requirements using a bundle of fibers as a yarn; one fiber would be a basic building block for large-scale devices. Other microsupercapacitors (or microbatteries) usually use thin-film technology, which would be difficult to scale up. Thus, our fiber supercapacitors could be scaled up easily and combined together with nanogenerators, which can charge the fiber supercapacitors. We will work on these tasks as a next step. The unique architecture of two fiber-based electrodes and use of  $\text{ZnO}$  NWs as an active material could be useful for the future development of flexible and wearable electronics. Furthermore, the method demonstrated herein would be applicable to develop other fiber-based devices, such as fiber-based microbatteries when flexibility and stretchability are required.

### Experimental Section

**ZnO NWs on plastic wire:** A PMMA wire was cleaned with deionized water, and deposited with 300 nm-thick gold film by using a radio-frequency magnetron sputter. Gold film on the wire was used as a seed layer to grow  $\text{ZnO}$  NWs and a charge collector for supercapacitors simultaneously. The growth of  $\text{ZnO}$  NWs on the wire was performed by using the typical hydrothermal growth method of  $\text{ZnO}$  NWs. The growth solution (2.5 mm) was prepared by dissolving zinc nitrate hexahydrate (98%, Aldrich) and hexamethylenetetramine (HMTA; 99%, Aldrich) in deionized water. The gold-coated plastic wires were then dipped in a glass bottle filled with the growth solution. The growth temperature was  $80^\circ\text{C}$ , and typical growth time was 18 h. The other electrodes were prepared using Kevlar 129 fibers as substrates. To grow  $\text{ZnO}$  NWs, the Kevlar fibers were deposited with  $\text{ZnO}$  thin film by using a radio-frequency magnetron sputter.  $\text{ZnO}$  NWs were then grown on the fibers by using the same procedures and growth conditions described above. Finally, a thin film of gold (ca.  $1 \mu\text{m}$  thick) was deposited on the  $\text{ZnO}$  NW to improve the charge collection performance of the electrodes for use as a supercapacitor. The surface morphology of  $\text{ZnO}$  NWs was characterized by using a field-emission scanning electron microscope (SEM, LEO 1550; Figure 1 e,f).  **$\text{MnO}_2$  coating:** First, a  $\text{KMnO}_4$  solution (6 mL, 0.1M) was prepared in the vial; the  $\text{ZnO}$  NWs-grown wire was then cut to the appropriate size (9 mm) and placed into the vial. Ultrasonication was performed to obtain better dispersion. Ethanol (6 mL) was then added into a vial dropwise under vigorous ultrasonication, and samples were taken out after 15 min.

Received: September 28, 2010

Published online: January 14, 2011

**Keywords:** fibers · nanowires · supercapacitors · zinc oxide

- [1] A. Kiebele, M. Kaempgen, G. Gruner, *Nanotechnol. Law Bus.* **2008**, 5, 7.
- [2] X. Fan, Z. Chu, F. Wang, C. Zhang, L. Chen, Y. Tang, D. Zou, *Adv. Mater.* **2008**, 20, 592.
- [3] J. R. McDonough, J. W. Choi, Y. Yang, F. L. Manita, Y. Zhang, Y. Cui, *Appl. Phys. Lett.* **2009**, 95, 243109.

- [4] P. Chen, G. Shen, S. Sukcharoenchoke, C. Zhou, *Appl. Phys. Lett.* **2009**, *94*, 043113.
- [5] U. Chung, C. Elissalde, S. Mornet, M. Maglione, C. Estournès, *Appl. Phys. Lett.* **2009**, *94*, 072903.
- [6] X. Wu, L. Jiang, F. Cao, Y. Guo, L. Wan, *Adv. Mater.* **2009**, *21*, 2710.
- [7] W. Sun, X. Chen, *J. Power Sources* **2009**, *193*, 924.
- [8] Y. Zhang, H. Li, L. Pan, T. Lu, Z. Sun, *J. Electroanal. Chem.* **2009**, *634*, 68.
- [9] D. Kalpana, K. S. Omukumar, S. S. Kumar, N. G. Renganathan, *Electrochim. Acta* **2006**, *52*, 1309.
- [10] P. Simon, Y. Gogotsi, *Nat. Mater.* **2008**, *7*, 845.
- [11] P. J. Hall, M. Mirzaeian, S. I. Fletcher, F. B. Sillars, A. J. R. Rennie, G. O. Shitta-Bey, G. Wilson, A. Cruden, R. Carter, *Energy Environ. Sci.* **2010**, *3*, 1238.
- [12] B. E. Conway, *Electrochemical Supercapacitors*, Kluwer-Academic, Dordrecht, **1999**.
- [13] K. Hung, C. Masarapu, T. Ko, B. Wei, *J. Power Sources* **2009**, *193*, 944.
- [14] M. Winter, R. J. Brodd, *Chem. Rev.* **2004**, *104*, 4245.
- [15] D. Pech, M. Brunet, H. Durou, P. Huang, V. Mochalin, Y. Gogotsi, P. Taberna, P. Simon, *Nat. Nanotechnol.* **2010**, *5*, 651.
- [16] Y. Qin, X. Wang, Z. L. Wang, *Nature* **2008**, *451*, 809.
- [17] Q. Wan, Q. H. Li, Y. J. Chen, T. H. Wang, X. L. He, J. P. Li, C. L. Lin, *Appl. Phys. Lett.* **2004**, *84*, 3654.
- [18] B. Weintraub, Y. G. Wei, Z. L. Wang, *Angew. Chem.* **2009**, *121*, 9143; *Angew. Chem. Int. Ed.* **2009**, *48*, 8981.
- [19] J. Goldberger, D. J. Sirbuly, M. Law, P. Yang, *J. Phys. Chem. B* **2005**, *109*, 9.
- [20] Z. L. Wang, J. Song, *Science* **2006**, *312*, 242.
- [21] Z. Zhao, S. R. Wang, C. You, *J. Intell. Mater. Syst. Struct.* **2010**, *21*, 1131.
- [22] C. J. Lee, T. J. Lee, S. C. Lyu, Y. Zhang, H. Ruh, H. J. Lee, *Appl. Phys. Lett.* **2002**, *81*, 3648.
- [23] H. J. In, S. Kumar, Y. Shao-Horn, G. Barbastathis, *Appl. Phys. Lett.* **2006**, *88*, 0831041.
- [24] D. Pech, M. Brunet, P. Taberna, P. Simon, N. Fabre, F. Mesnilgrete, V. Conédéra, H. Durou, *J. Power Sources* **2010**, *195*, 1266.
- [25] M. Kaempgen, C. K. Chan, J. Ma, Y. Cui, G. Gruner, *Nano Lett.* **2009**, *9*, 1872.
- [26] S. Xu, C. S. Lao, B. Weintraub, Z. L. Wang, *J. Mater. Res.* **2008**, *23*, 2072.
- [27] J. Jiang, A. Kucernak, *Electrochim. Acta* **2002**, *47*, 2381.
- [28] H. Y. Lee, J. B. Goodenough, *J. Solid State Chem.* **1999**, *144*, 220.
- [29] V. Subramanian, H. W. Zhu, B. Q. Wei, *Electrochem. Commun.* **2006**, *8*, 827.